Investigation of a composite ring rolling process by FEM and experiment

Joachim Seitz[1,a], Gideon Schwich[1], Stefan Guenther[1] and Gerhard Hirt[1]

[1]*IBF-Institute of Metal Forming, RWTH Aachen University, Intzestraße 10, 52056 Aachen, Germany*

Abstract. Roll bonding is a well-known process to produce composite sheet metals. Transferring this principle to ring rolling would allow to produce seamless radial composite rings, which combine the advantages of different material properties. This process is studied, both experimentally and using FEM-simulation. For the FEM an explicit model is applied including the kinematic control algorithms of the radial-axial ring rolling machine. In the used model the occurrence of unexpected asymmetrical joints can be reproduced, which are observed during the rolling experiments. By varying the influencing parameters on the asymmetric joint in the FEM a plausible reason was found.

1 Introduction

Ring rolling is an incremental bulk metal forming process for manufacturing seamless rings of different diameters and cross-sections. Seamless rings are typically used in bearing, aircraft, energy, and automotive industry [1]. The conventional radial-axial ring rolling process holds eight degrees of freedom and reduces the cross-section of a ring within two roll gaps. The radial roll gap consists of a rotatory driven main roll (1) and a non-driven mandrel (2), which moves in the direction of the main roll to reduce the wall thickness. Two rotationally driven conical axial rolls (3, 4) constitute the axial roll gap, which is located opposite to the radial roll gap. The upper axial roll moves vertically downwards to the lower one (5) reducing the ring height. The axial rolls are fixed in the axial frame (6), which can move in radial direction with growing ring diameter. Two guide rolls control the position of the ring (7, 8) and ensure its circularity during the process. The guide rolls are situated at the side of the ring [1]. Figure 1 provides a schematic overview of the radial-axial ring rolling process.

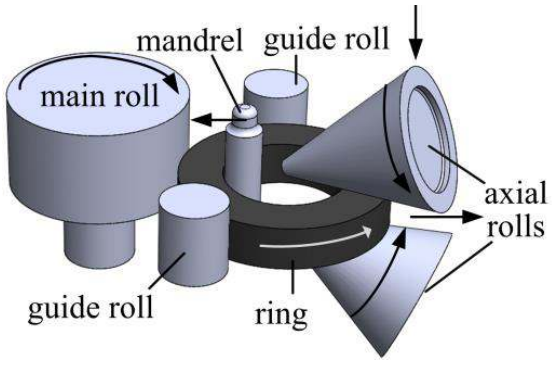

Figure 1. Schematic representation of the radial-axial ring rolling process.

Composite materials provide the opportunity to satisfy locally variable material demands by combining the respective advantages of different materials in one workpiece. This combination of materials enables customized material properties. Through the combination of high quality materials with low-cost materials the component costs can be reduced. Within this investigation metallic seamless composite rings are considered, where the bonding mechanism is characterized by a material bond. While today roll-bonding is a basically established technology for producing planar semi-finished products [2], the manufacturing of composite rings by ring rolling is only poorly studied[3, 4]. In order to enable the manufacture of composite rings by ring rolling, the relevant correlations between process parameters and material properties have to be identified and described by models.

Within this paper, first findings of the material flow are presented based on investigations by ring rolling experiments as well as further investigations using FEM-simulations. Using FEM-models will enable to derive suitable rolling strategies and to identify valid process windows for a reliable and reproducible formation of a material bond by ring rolling.

2 State of the Art

2.1 Metallic composites joined by a material bond

Apart from all kinds of surface coating, the basic concept of metallic composite materials by material bonding can amongst others be realized by roll bonding [5], composite casting, composite forging [6], cladding [7], powder metallurgy [3, 8] and modern additive manufacturing. For thin material bonded coatings, various thermal spraying processes are industrial state of the art. Thermal spraying

[a] Corresponding author: seitz@ibf.rwth-aachen.de

can be divided according to the type of spray additive material, to the production process and according to the type of energy source (e.g. plasma spraying, flame spraying, laser spraying). However, the achievable layer thicknesses are limited to a few millimeters [9]. In contrast, composite materials with relatively thick layers can be achieved by cladding, for which various fusion welding methods are available [7]. In particular for high alloyed high-temperature materials problems like hot cracks, shrinkage cracks and diffusion-related alloy changes are observed. In general, the thermal coating of layers is limited with respect to the coating rate and therefore more suitable for smaller volumes.

Rotationally symmetrical seamless hollow composites can be produced by centrifugal casting processes [10]. However, for this process an accumulation of nonmetallic inclusions and less dense components such as oxides, slag and gases on the inside can occur due to the centrifugal force and the solidification direction. These nonmetallic inclusions generate a harmful segregation layer, which is difficult to remove for the composite casting because the second (inner) layer should be casted immediately after the solidification of the first to achieve a good metallic bond between the layers [11]. In summary, all melt metallurgical processes cause "cast structures" in the broader sense with the associated microstructures and the adverse mechanical properties compared to forming processes.

Various forming or thermal joining processes for rotationally symmetrical parts exist, in which the composite is mainly realized by force fit or material bonding. For example, seamless composite pipes are produced by hydroforming (wall thickness about 10 mm, outer diameter about 150 mm), where the resultant composite is realized by force fit. This process is amongst others used in the chemical industry [12].

The generation of material bonded composites for seamless tubular semi-finished products by forming processes can be carried out using more recent approaches like the simultaneous extrusion of different metals [13] or the joining by metal spinning (so-called "spin-bonding") [14]. Seamless composite rings can also be produced by a process-integrated powder coating during the radial-axial ring rolling process. In this case, the powder substrate is filled into a previously welded capsule space. Here, the process steps compacting, forming and heat treatment are carried out simultaneously during the ring rolling. Depending on the composition of the coating powder, a wear and / or corrosion-resistant layer can be obtained [3]. For this process, the advantage of reducing the necessary production steps is accompanied by the high procedural effort for attaching the necessary capsule space. In addition, for a large ring growth cracks can occur in the coating during the forming process, which significantly limit the process window compared to conventional ring rolling. Despite the compression by rolling, residual porosity is not completely avoidable and the achievable coating thickness is limited.

Roll bonding is probably the most industrially established and quantitatively widespread method for producing material bonded composites [2] and it has many analogies to the composite ring rolling. Roll bonding is a pressure welding process, which requires a close contact and a high pressure of the materials to be joined. Inserting forming energy into the contact area initializes a material bond of the composite layers at the atomic level [5, 15]. Roll bonding is used in cold and hot rolling, wherein the clad can by realized both by reversible and continuous rolling. As described by Bay in [15], roll bonding enables the realization of metal combinations, which cannot be bonded by melting processes due to the formation of intermetallic phases. The application areas of hot roll bonded composites are mainly the chemical industry, where corrosion resistant materials are combined with low-cost construction materials. Thin layered composites are mainly used in the automotive industry, electrical industry and heat technology. Here, material properties such as electrical and thermal conductivity or corrosion resistance of non-ferrous metals are combined with the strength of steel or other alloys [16].

Transferring the concepts of roll bonding to radial-axial ring rolling could basically allow producing seamless composite rings with outer diameters up to 9,500 mm and ring heights up to 4,000 mm with individual weights up to 150 tons [1]. The composite ring rolling has hardly been studied, although all other joining methods are not suitable for these target geometries by forming processes. Therefore, the process is not applied in industry yet.

The composite ring rolling of concentrically arranged rings has been studied as an aspect of a research project in the early 1990s [4]. Figure 2 provides a schematic representation of the composite ring rolling process. As a result of the investigations, it was postulated that the inner ring has to grow faster than the outer ring. This requirement has to be satisfied for the creation and maintenance of a material bond. The flow resistance is the parameter to evaluate when plastic deformation and therefore ring growth occurs. The flow resistance in the circumferential direction depends on the flow stress of the material σ_y as well as on the radial shape factor c_r (ratio of contact length l_D to the wall thickness s of the ring, cf. chapter 4). Consequently, for the use of materials with different strengths, the higher strength material should be located outside.

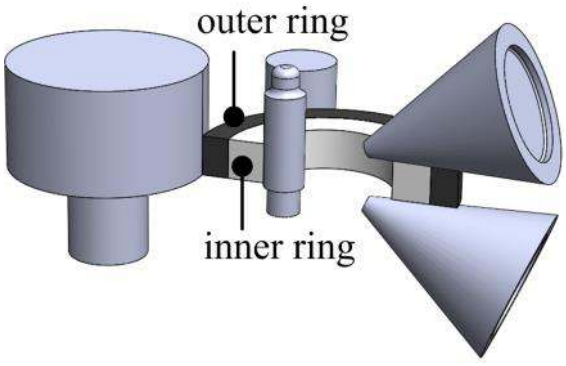

Figure 2. Schematic representation of the composite ring rolling process of concentrically arranged rings.

2.2 FEM-simulation of the ring rolling process

The analysis of local stress and strain states and the thermal conditions is required in order to investigate the elaboration of a material bond in composite ring rolling. Due to the asymmetrical and transient process conditions this can only be achieved by the finite element method.

As a result of the increased computing power and more efficient contact algorithms, today ring rolling can be simulated using FEM with both implicit [17, 18] as well as with explicit solution methods [19]. The FEM-simulation of the radial-axial ring rolling process uses increasingly integrated closed-loop control algorithms for most or all of the at least eight degrees of freedom. The control algorithms of the simulation are based on the process control of real ring rolling machines using virtual sensors to measure current process information. Based on this approach, no additional information from previously conducted rolling experiments are required anymore. In some publications the controlled kinematics of the guide rolls are described in the model [19–22]. Also some approaches for a force control of the guide rolls were realized, using hydraulic cylinders as drives for the centering arms [21]. Successively all eight degrees of freedom have been automated through the implementation of virtual sensors and control algorithms [23]. Since the control algorithms of the ring rolling mills belong to the protected know-how of the supplier, in past investigations of the IBF [24, 25] the control algorithms were implemented in a first step as a black box provided by the machine supplier. In a further step, own fully documented control algorithms were integrated into the FEM-simulation. The existing FEM-simulation model allows ring rolling processes without prior knowledge of the expected kinematics as well as the development of new rolling strategies [24, 25].

3 Methods and procedure

3.1 Experimental equipment

The rolling experiments were conducted on a radial axial ring rolling mill Banning H100/V80 with a maximal radial force of 1000 kN and a maximal axial force of 800 kN. For the conducted experiments the materials 1.7131 (inner ring) and 1.4401 (outer ring) were used. The rings were heated up to 1200°C and held at 1200°C for 90 min. The transport time was approx. 60 s and the process time approx. 15 s.

3.2 Description of the FEM-model

The flow curves of the materials are determined using frictionless isothermal single step compression tests at different strain rates and temperatures for the above mentioned two materials. The determined flow curve data are stored in tabular form depending on the strain rate, the temperature and the equivalent strain. Therefore isotropic hardening as a function of strain, strain rate and temperature is considered. The dependency on strain rate and temperature is covered by linear interpolation between experimental values measured at $d\varepsilon/dt = 0{,}01/s$, 0,1/s, 1/s, up to 10/s and temperatures between $\vartheta = 950°C$ and 1200°C in steps of 50°C. The additional material data, such as density, Young's modulus, specific heat capacity and thermal conductivity were taken from literature [26]. The simulation uses a thermo-mechanical coupled model with an explicit solver in ABAQUS. Between the tools and the rings, as well as between the rings among each other a "surface to surface" contact condition is defined using a "hard contact" condition in normal direction and a Coulombian friction coefficient of $\mu = 0.3$ in tangential direction. The ring temperature at the beginning of the process is $\vartheta_{0,ring} = 1200$ °C and the tool temperatures are $\vartheta_{tool} = 100°C$ throughout the process. The two rings are meshed each with approx. 7500 hexahedral reduced elements (C3D8RT) using an ALE formulation. The simulation considers gravity and the existence of a rolling table. The conducted simulations use a fully closed-loop controlled model, which is described in detail in [24, 25]. The control loop for the eight degrees of freedom is realized in FORTRAN via an ABAQUS user subroutine called VUAMP. Figure 3 shows the basic structure of the control loop and the FEM-simulation model containing all the used virtual sensors and actuators.

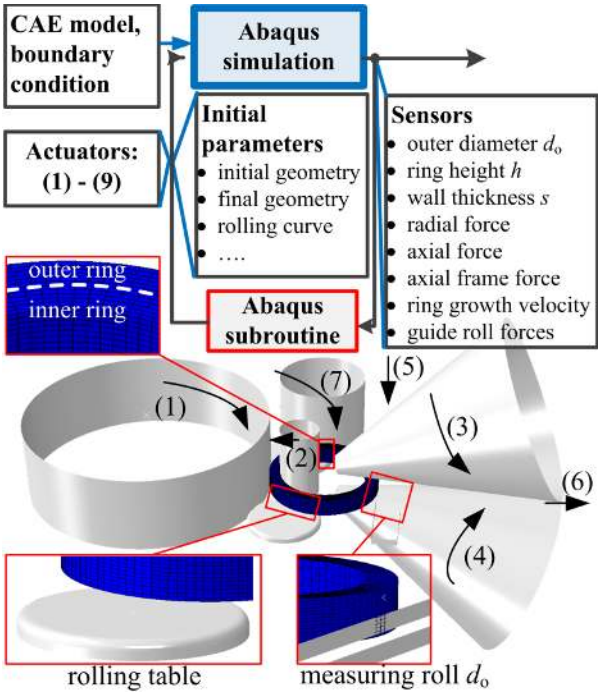

Figure 3. FEM-model of the composite ring rolling process with integrated closed-loop control.

4 Results and Discussion

In order to enable the formation of a permanent material bond by ring rolling the inner ring has to grow faster than the outer ring.

Considering the material, the following condition must be satisfied: The forming resistance of the inner ring close to the mandrel is less than that of the outer ring next to the main roll. To satisfy this condition, a material

combination of a case hardening steel 1.7131 (inner ring) and an austenitic stainless steel 1.4401 (outer ring) was examined. The difference of the two flow stresses increases with decreasing temperature and with increasing equivalent strain. Therefore the difference increases during the ring rolling process. Figure 4 provides an exemplary comparison of the flow curves of the inner ring and the outer ring at two different temperatures, which point out the increasing difference with decreasing temperature.

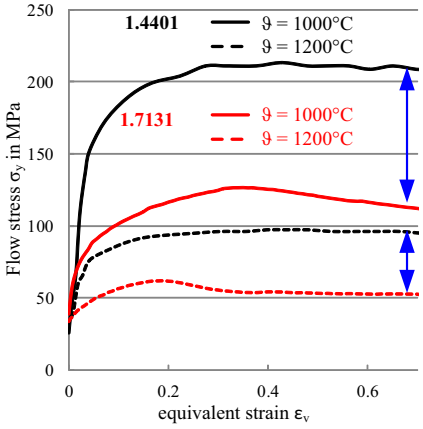

Figure 4. Exemplary comparison of flow curves of the inner ring (1.7131) and the outer ring (1.4401) for a strain rate of $d\varepsilon/dt = 1/s$ at the temperatures $\vartheta = 1000°C$ and $\vartheta = 1200°C$.

In addition, the choice of the mandrel diameter and the inner diameter of the preform is restricted based on geometrical considerations. The basic requirement is that the contact length l_M of the main roll has to be at least as large as the contact length of the mandrel l_D, since an increase of the contact length effects a higher ring growth rate. The concept of contact length is transferred from conventional flat rolling, where l_c is a function of the height reduction $\Delta h = (h_1\text{-}h_0)$ and the roll radius r. Figure 5 provides the concept of contact length l_c and shape factor c_s for conventional flat rolling.

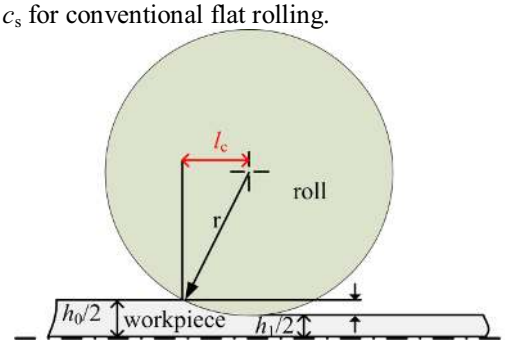

Figure 5. Concept of contact length l_c and shape factor $c_s = l_c/[(h_1+h_0)/2]$ for conventional flat rolling.

In ring rolling, the geometric relationships of radial shape factor and contact length are more complex due to the curvature of the ring, the different diameters of main roll and mandrel as well as the diameter increase of the ring. Therefore, a notional diameter of the main roll d'_M and the mandrel d'_D, which depends on the current ring diameter and the tool geometry can be calculated according to [27] through the entire process.

Figure 6 provides the evolution of the measured outer diameter d_o, the inner diameter d_i and the calculated evolution of the notional diameters of the main roll d'_M and the mandrel d'_D for the performed rolling operations (used mandrel roll diameter $d_D = 75$ mm, main roll diameter $d_M = 748$ mm). Since the notional diameter of the mandrel d'_D is reduced with increasing ring outer diameter d_o whereas the notional diameter of the main roll d'_M is increased, it is possible to determine a valid preform based on fixed tool dimensions, which satisfy the geometrical requirement for the entire process.

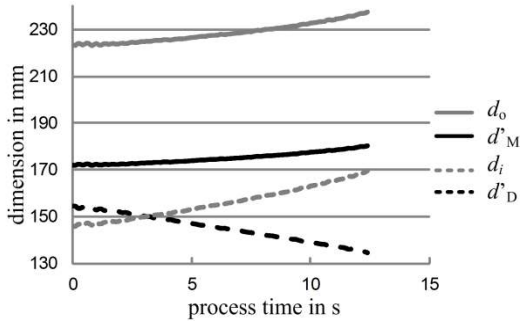

Figure 6. Evolution of the measured diameters d_o and d_i and the notional diameters d'_D and d'_M.

Figure 7 provides valid preform geometries for two different mandrel diameters according to the described geometrical considerations. The area above the dashed line of one color, which corresponds to one mandrel diameter, can be chosen for the inner diameter of the preform. The outer diameter can be determined by adding twice the total wall thickness to the inner diameter. In this Figure, the wall thicknesses of the inner and outer ring are equal.

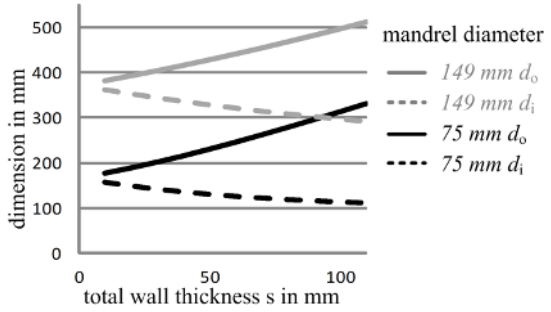

Figure 7. Process window for the choice of the preform geometry using different mandrel diameters.

Based on the above mentioned considerations, the following preform geometries were selected, in order to induce a higher ring growth of the inner ring compared to the outer ring.

Table 1. Chosen preform and final geometries

$d_D = 75$mm	preform outside	preform inside	final geometry
d_o in mm	217	177	242
d_i in mm	177	136	174
h in mm	39	39	39

4.1 Results of rolling experiments and FEM-simulations

The results of the first rolling experiments and FEM-simulations using a mandrel diameter of $d_D = 75$ mm show that an excessive ring growth of the inner ring can be harmful. In this case, the inner ring grows too fast compared to the outer ring, so the inner ring outgrows the outer one. In consequence, the two rings are separated. Figure 8 shows the final geometries of the first rolling experiments in reality and FEM-simulation. This first result already shows that a reproducible successful control of composite ring rolling requires additional process boundaries to the above mentioned considerations, which will be examined within the running research.

Figure 8. Final geometries in case, the inner ring grows too fast and outgrows the outer ring. left: rolling experiment right: FEM-simulation**.**

In the subsequent rolling experiments the inner diameter of the inner ring has been reduced and a larger mandrel diameter of d_D = 120 mm has been selected, which increases the notional diameter of the mandrel d'_D. This leads to a smaller ring growth of the inner ring.

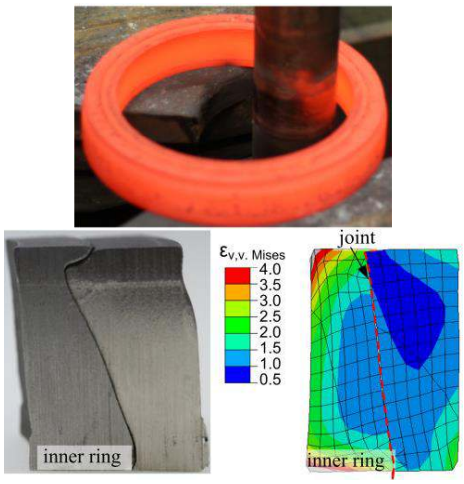

Figure 9. Composite ring after rolling. left: cross section of the rolled ring, right: Cross-section of the rolled ring in FEM.

According to a first examination of the rolled ring, which is provided in Figure 9, it can be assumed that the flow behavior satisfies all the requirements for an adequate material bond. However, a radial cut of the rings shows that the material flow of the inner ring and the outer ring is not uniform in axial direction. This phenomenon can also be reproduced in the FEM-simulation (see Figure 9). In addition, the resulting composite has no sufficient bonding and can be separated manually. In order to understand the reason for asymmetrical joints and the influence of process parameters, FEM-simulations have been conducted.

4.2 Influence of the ratio between wall thickness and ring height

It is known from flat rolling that the tendency of spreading increases with increasing shape factor c_s (ratio of contact length to height of the workpiece) and with decreasing width-to-height ratio b_m / h_m. In order to investigate the influence of the width-to-height ratio b_m / h_m in the radial roll gap, the height of the rings was varied using otherwise unchanged rolling conditions. Transferring the conditions of flat rolling to the radial roll gap of the ring rolling process, the ring height corresponds to the width of the workpiece b_m (the dimension perpendicular to the roll feed). In all ring rolling processes the ring height was kept constant by the axial rolls during the process. Figure 10 shows the final cross-sectional geometry for three different initial and final ring heights. The lower the ratio of height to wall thickness of the ring, the more asymmetric the joint becomes.

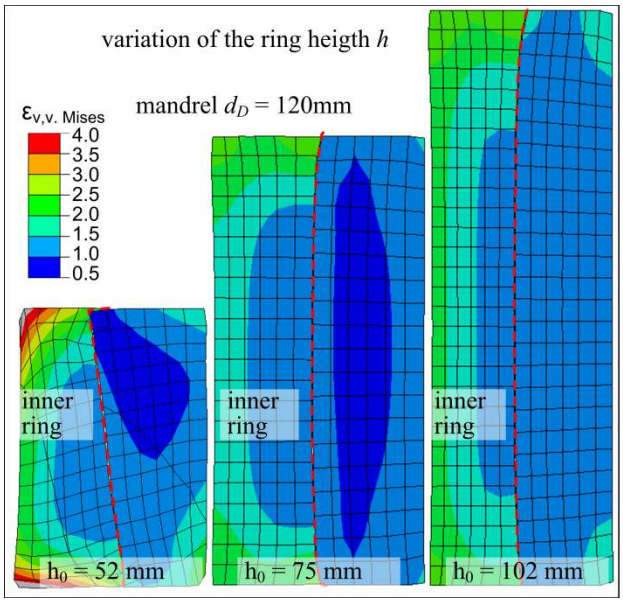

Figure 10. Final cross-sections for different ring heights *h*.

4.3 Influence of the flow stress ratio between inner and outer ring and the mandrel diameter

In order to investigate the influence of the flow stress ratio between inner and outer ring on the asymmetric joint, notional flow curves have been used for the inner ring. These flow curves were generated using a scaled flow curve of the outer ring (1.4401) by factor 100%, 90%, 80% and 70%. This flow curve variation was performed for two different mandrel diameters of $d_D = 75$ mm and $d_D = 120$ mm. Figure 11 provides the cross-sections at the end of the rolling process. The smaller the notional diameter of the mandrel d'_D and the lower the flow stress, the earlier the inner ring starts growing plastically compared to the outer ring and the more asymmetric is the formed joint.

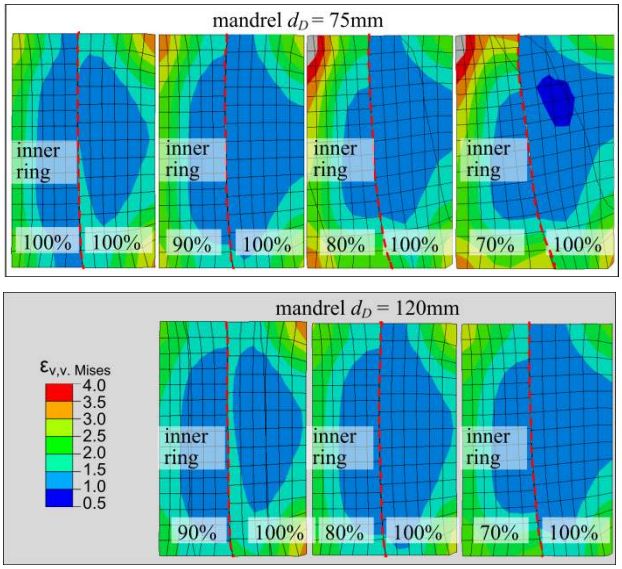

Figure 11. Comparison of the final cross-sections for the variation of the flow stress of the inner ring relative to the flow stress of the outer ring (precentage values) at the example of two mandrel roll diameters.

4.4 Influence of the rolling table and the gravity

After having determined how the occurring asymmetrical joints may be affected, the reason for its occurrence is still unknown. In order to find the reason, successively the conditions, which act in different ways up and downwards, were excluded keeping all other conditions constant. Random process disturbances or different tool stiffnesses of the axial rolls by differences in the guiding of the axial slide can be excluded, since the tools are modelled in FEM as rigid bodies and the asymmetrical joint can be reproduced by the FEM-model. The two remaining asymmetric boundary conditions are gravity and the rolling table. In Figure 12, the final cross-sections of three FEM-simulations are shown, in which the above mentioned influencing parameters were investigated. Accordingly, the rolling table is the reason for the asymmetrical joint.

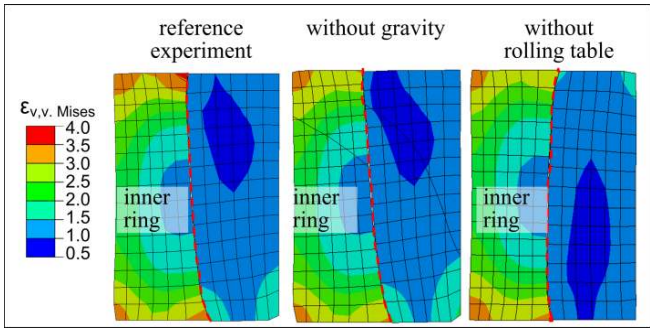

Figure 12. left: final cross-section of the reference experiment, taking into account gravity and the rolling table, center: without considering gravity with rolling table**,** right**:** without rolling table with gravity.

5 Conclusion and Outlook

Composite materials provide the opportunity to realize customized material properties by combining the advantages of different materials in one workpiece. The producible layer thicknesses in composite ring rolling are not limited unlike the industrially established processes for seamless composite rings. The composite ring rolling process allows joining and forming in only one process.

In this paper a FEM-model for the composite ring rolling using simple contact algorithms was developed. This model provides important information on the stress and strain state, i.e. the radial and tangential material flow. The results of the investigations show that simple analytical considerations are not sufficient for the process layout and a reproducible realization of composite ring rolling. Even composite rolling experiments, which seem to be successful according to a first consideration, not necessarily meet the required demands on a uniform material distribution or a specific joint strength. Notably, the following effects are observed:

- The inner ring may outgrow from the outer ring
- No sufficient material bond
- Occuring of an asymmetric joint, which can be influenced by:
    - The chosen material (flow stress) combination of the rings
    - The ratio of wall thickness to ring height
    - The existence of a rolling table

The realized investigations generate first relationships between preform, tool geometries and the expected ring growths. Nevertheless, no criteria are known yet for describing these process boundaries qualitatively or even quantitatively. For a reproducible material bond with thick wall thicknesses and large diameters by composite ring rolling a detailed understanding of all influencing parameters of the material flow and the bond formation is required.

The focus of future investigations will therefore concentrate on modelling the resulting joint strength in the FEM. For this purpose it will be necessary to extend the ring rolling model to a contact formulation that considers the material bond creation.

Acknowledgement

The authors would like to thank the “Deutsche Forschungsgemeinschaft” (DFG) for the financial support of these works within the project HI 790/54-1 “Verbundringwalzen - Methode zur Herstellung nahtloser Verbundringe auf einem Radial-Axial Ringwalzwerk”.

References

1. U. Koppers, D. Michl, in Handbuch Umformen, ed. by H. Hoffmann, R. Neugebauer, G. Spur (Hanser München, 2012), p. 187
2. Roll-bonded clad plates: our cost-efficient answer to corrosion (Linz) (https://www.voestalpine.com/division_stahl/conten

t/download/4248/34321/file/Folder_Roll-bonded-clad-plates_E_291014.pdf)
3. R. Kebriaei, J. Frischkorn, S. Reese, T. Husmann, H. Meier, H. Moll, W. Theisen, J. Mater. Process. Technol. 213, 2015 (2013)
4. A. Kluge, H. Wiegels, R. Kopp, Stahl und Eisen, 37 (1995)
5. R. Jamaati, M.R. Toroghinejad, Mater. Sci. Technol. 27, 1101 (2011)
6. B.-A. Behrens, K.-G. Kosch, Mat.-wiss. u. Werkstofftech. 42, 973 (2011)
7. H.J. Fahrenwaldt, H. Schuler, J. Twrdek, Praxiswissen Schweißtechnik - Werkstoffe, Prozesse, Fertigung (Springer Vieweg, Wiesbaden, 2014)
8. H.V. Atkinson, S. Davies, Metall. and Mat. Trans. A 31, 2981 (2000)
9. L. Pawlowski, The science and engineering of thermal spray coatings (Wiley, Chichester, England, Hoboken, NJ, 2008)
10. M. Eitschberger, C. Körner, R.F. Singer, in Verbundwerkstoffe und Werkstoffverbunde, ed. by B. Wielage, G. Leonhardt (Deutsche Gesellschaft für Matrialkunde e.V. Weinheim, 2001), p. 114
11. P. Kapranos, C. Carney, A. Pola, M. Jolly, in Comprehensive Materials Processing (Elsevier, 2014), p. 39
12. X. Wang, P. Li, R. Wang, Int. J. Mach. Tool Manu. 45, 373 (2005)
13. L. Madej, H. Paul, L. Trebacz, W. Wajda, M. Pietrzyk, CIRP Annals - Manufacturing Technology 61, 235 (2012)
14. M.S. Mohebbi, A. Akbarzadeh, J. Mater. Process. Technol. 210, 510 (2010)
15. N. Bay, H. Bjerregaard, S.B. Petersen, C. dos Santos, J. Mater. Process. Technol. 45, 1 (1994)
16. Plattiertes Stahlblech: Merkblatt 383
17. M. Ramadan, L. Fourment, H. Digonnet, Int J Mater Form 2, 581 (2009)
18. H. Schafstall, C. Barth, in Proceedings of the 13th International Conference on Metal Forming, ed. by Steel research international (Stahleisen GmbH Düsseldorf, 2010), p. 202
19. M. Wang, H. Yang, Z. Sun, L. Guo, X. Ou, Trans. Nonferrous Met. Soc. China 16, 1274 (2006)
20. Z.W. Wang, S.Q. Zeng, X.H. Yang, C. Cheng, J. Mater. Process. Technol. 182, 374 (2007)
21. L. Li, H. Yang, L. Guo, Z. Sun, J. Mater. Process. Technol. 1-3, 205 (2008)
22. L. Guo, H. Yang, M. Zhan, H. Li, L. Li, Materials Science Forum, 471-764 (2004), p. 760-764
23. Z. Wang, J. Fan, D. Hu, C. Tang, C. Tsui, Int. J. Mech. Sci., 52, (2010), p. 1325-1333
24. V. Jenkouk, G. Hirt, M. Franzke, T. Zhang, CIRP Annals - Manufacturing Technology 61, 1 (2012)
25. V. Jenkouk, G. Hirt, J. Seitz, AIP Conference Proceedings 1532, 695 (2013)
26. M. Spittel, T. Spittel., Materials, Landolt-Boernstein - Group VIII Advanced Materials and Technologies Volume 2, 98/162 (2009)
27. U. Koppers, Geometrie, Kinematik und Statik beim Walzen von Ringen mit Rechteckquerschnitten. Dissertation (Aachen, RWTH) (1987)